NIH Public Access
Author Manuscript
Mol Cancer Ther. Author manuscript; available in PMC 2014 July 01.

Published in final edited form as:
Mol Cancer Ther. 2013 July ; 12(7): 1299–1309. doi:10.1158/1535-7163.MCT-12-0968.

Drug Repurposing for Gastrointestinal Stromal Tumor

Ziyan Y. Pessetto[1], **Scott J. Weir**[2,3,6], **Geetika Sethi**[1,4], **Melinda A. Broward**[3,5,6], and **Andrew K. Godwin**[1,6]

[1]Pathology & Laboratory Medicine, University of Kansas Medical Center, Kansas City, Kansas

[2]Department of Pharmacology, Toxicology and Therapeutics, University of Kansas Medical Center, Kansas City, Kansas

[3]Institute for Advancing Medical Innovation, University of Kansas Medical Center, Kansas City, Kansas

[4]Department of Biochemistry, Drexel University College of Medicine, Philadelphia, PA

[5]Lead Development and Optimization Shared Resource, High Throughput Screening Laboratory, University of Kansas, Lawrence, Kansas

[6]University of Kansas Cancer Center, Kansas City, Kansas

Abstract

Despite significant treatment advances over the past decade, metastatic gastrointestinal stromal tumor (GIST) remains largely incurable. Rare diseases, such as GIST, individually affect small groups of patients but collectively are estimated to affect 25–30 million people in the U.S. alone. Given the costs associated with the discovery, development and registration of new drugs, orphan diseases such as GIST are often not pursued by mainstream pharmaceutical companies. As a result, “drug repurposing” or “repositioning”, has emerged as an alternative to the traditional drug development process. In this study we screened 796 FDA-approved drugs and found that two of these compounds, auranofin and fludarabine phosphate, effectively and selectively inhibited the proliferation of GISTs including imatinib-resistant cells. One of the most notable drug hits, auranofin (Ridaura®), an oral, gold-containing agent approved by the FDA in 1985 for the treatment of rheumatoid arthritis (RA), was found to inhibit thioredoxin reductase (TrxR) activity and induce reactive oxygen species (ROS) production, leading to dramatic inhibition of GIST cell growth and viability. Importantly, the anti-cancer activity associated with auranofin was independent of IM resistant status, but was closely related to the endogenous and inducible levels of ROS, therefore is prior to IM response. Coupled with the fact auranofin has an established safety profile in patients, these findings suggest for the first time that auranofin may have clinical benefit for GIST patients, particularly in those suffering from imatinib-resistant and recurrent forms of this disease.

Keywords

drug repurposing; drug repositioning; auranofin; gastrointestinal stromal tumors treatment; thioredoxin reductase activity

Corresponding Author: Andrew K. Godwin, PhD, University of Kansas Medical Center, 4005B Wahl Hall East, 3901 Rainbow Boulevard Kansas City, KS 66160. Phone: 913-945-6373; Fax: 913-945-6327; agodwin@kumc.edu.

Conflicts of Interest Statement: The authors declare no conflict of interest.

NIH-PA Author Manuscript
NIH-PA Author Manuscript
NIH-PA Author Manuscript

NIH-PA Author Manuscript

NIH-PA Author Manuscript

NIH-PA Author Manuscript

INTRODUCTION

Gastrointestinal stromal tumors (GISTs) are the most common mesenchymal malignancies of the digestive tract with an estimated annual incidence of ~6,000 new cases in the United States (1). Approximately ~85% of GISTs contain somatic activating mutations in one of two proto-oncogenes: *KIT* or *PDGFRA*, which encode the tyrosine kinase receptors c-KIT and the platelet-derived growth factor receptor α, respectively (2–4). More recently, mutations in the serine-threonine kinase *BRAF* have been identified in a very small number of GISTs (5, 6).

Historically, there were few safe and effective therapeutic options for long-term GIST treatment and disease maintenance due to the ineffectiveness of radiation and cytotoxic chemotherapy. The clinical outlook for adults with GIST improved radically following the discovery that this malignancy is most commonly driven by signaling via the c-KIT receptor, which can be inhibited by small molecule tyrosine kinase inhibitors such as imatinib (7–10). In a series of clinical trials, treatment of advanced-stage patients with imatinib yielded objective response rates of 55–78%, with approximately half of patients remaining disease-free for 2 years and median overall survival of approximately 50–55 months (11). Imatinib also delayed time to disease progression in the adjuvant setting, with a trend toward improved overall survival. These data led FDA to approve imatinib for treatment of advanced-stage GIST in 2002, and for use in the adjuvant setting in 2008.

Unfortunately, resistance to imatinib has been increasingly observed (8, 11–13). Resistance to initial therapy, so-called `early' or `intrinsic' resistance, occurs in 10–20% of patients; late, or `acquired' resistance, occurs in about 40% of patients. The molecular mechanisms of both categories of resistance are being elucidated including secondary mutations in *c-KIT* or *PDGFR*, leading to the introduction of newer kinase inhibitors targeting these additional pathways into the clinic. However, it is now also clear that GIST cells can utilize complex, redundant mechanisms to maintain aberrant signaling, which may confound therapy with drugs targeting any particular kinase (4, 8, 14, 15).

Recently, a putative GIST stem cell (KITlowCd44+Cd34+) has been identified (16, 17). These GIST stem cells, which have the potential to completely reconstitute tumors and establish metastases, are inherently resistant to inhibitors of c-KIT and PDGFR. Thus, the next generations of therapies for GIST will almost certainly have to include other drugs with independent, potentially complementary mechanisms of action to currently-used kinase inhibitors (18).

Costs associated with the discovery, development and registration of novel, new drugs have been estimated in excess of $1.5 B and require 10–17 years to complete. As a result, rare or orphan diseases such as GIST are often not pursued by large, for-profit pharmaceutical companies. In recent years, *drug repurposing*, identifying new therapeutic applications for FDA approved and abandoned drugs, has been demonstrated as a successful approach to addressing the unmet medical needs of patients suffering from rare diseases. Novel approaches to *drug rediscovery*, the identification of opportunities to evaluate FDA approved and abandoned drugs for new therapeutic uses, have emerged. Patients gain access to promising new therapies much more quickly by capitalizing on prior experience, resulting in reduced drug development and registration cycle times and cost (19). By employing *repurposing* and *rediscovery* strategies, drug development becomes affordable and achievable by non-profit organizations including academia, government, and disease philanthropy organizations, particularly through creative partnerships (20).

We report a drug repurposing approach to identify a potential drug for GIST patients. Auranofin inhibits TrxR enzymatic activity and increases ROS production. Auranofin

NIH-PA Author Manuscript

NIH-PA Author Manuscript

NIH-PA Author Manuscript

treatments lead to early and late apoptosis in GIST cells that result in cell death. In summary, we have shown that inhibition of GIST cell proliferation and induction of apoptosis by auranofin is dependent on drug-induced changes in ROS production.

MATERIALS AND METHODS

General Methods

All cell proliferation and caspase activity measurements were made on 384-well, black μClear microplates (Greiner bio-one, Germany). All cell proliferation experiments were assessed using the CellTiter-Blue® reagent according to the manufacturer's protocol (Promega). All fluorescence or luminescence measurements were made using Infinite® M200 Pro plate reader (Tecan, Switzerland). The fluorescence values are reported in relative fluorescence units (RFU) and were measured at an excitation wavelength of 544 nm and an emission wavelength of 590 nm. Data were normalized to percentage inhibition and IC_{50} concentrations were determined for each drug over a 72-h incubation period by the SigmaPlot program (Systat Software).

Compound Library

The FDA-approved drug Library (provided by the Lead Development and Optimization Shared Resource within the NCI Cancer Center at the University of Kansas) contains 796 drugs with known bioavailability and safety in humans. Compounds were present at 10 mM in DMSO. The full list of drugs is provided in Table S1. For hit validation, IM was purchased from the LC Laboratories and dissolved in sterile water. Fludarabine phosphate, idarubicin HCl, and bortezomib were purchased from the Selleck Chemicals. All drugs except IM were dissolved in DMSO.

Cell Culture

GIST-T1, a tumor cell line possessing a heterozygous mutation in *KIT* exon 11, was kindly provided by Takahiro Taguchi and untransformed smooth muscle cell line ULTR cells were purchased from ATCC and maintained in DMEM containing 10% fetal bovine serum (14). GIST 882 cells (c-*KIT* exon 13 homozygous mutation) were gifted from Jonathan A Fletcher and maintained in RPMI containing 15% fetal bovine serum (21, 22). GIST T1-10R cells, derived in Dr. Godwin's laboratory, were maintained in DMEM containing 10% fetal bovine serum and supplied with 10 μM IM to maintain drug resistance. IM was deleted from the culture for indicated hours in experiments with GIST T1-10R cells. Hs 919.T. cells were purchased from ATCC and maintained in DMEM containing 10% fetal bovine serum. All cell lines were supplied with 1% penicillin/streptomycin and were maintained in a 5% CO_2 atmosphere at 37 °C. Authentication for cell lines that were not purchased from ATCC was carried out by the Clinical Molecular Oncology Laboratory (The University of Kansas Cancer Center, KS USA).

Quantitative Drug Screen Assay

Drugs or vehicle (DMSO) were preloaded by the KU High Throughput Screen Laboratory (KU HTSL) as 250 nL aliquots on an Echo550 platform to each well to give a final doses range from 10 μM to 0.078 μM (serial twofold dilutions) in 25 μl in duplicates (38 plates for each cell line). Cells were grown to 80% confluence, harvested and aliquoted into 384 well plates at concentrations of 1,000–1,500 cells per well in a total volume of 25 μl/well with or without imatinib mesylate using a Matrix Wellmate (Thermo Scientific). The imatinib mesylate concentrations used for the combination study were the IC_{30} values: 10 nM, 10 nM, and 40 nM for GIST-T1, GIST T1-10R, and GIST 882 cells respectively (data not shown). Cells were cultured for 72 hours at 37 °C. Aliquots of 5 μl CellTiter-Blue®

NIH-PA Author Manuscript

NIH-PA Author Manuscript

NIH-PA Author Manuscript

Reagent were added directly to each well, the plates were incubated at 37 °C for 3 h and the fluorescent signal was measured. IM-treated (at established IC_{50} value for each cell line) wells and vehicle only wells on each plate were uniformly distributed throughout the screen and served as intraplate controls. Background plates containing vehicle only were inserted throughout the screen as interplate controls. The controls were used to calculate the background levels of the assay and to evaluate assay response as well as performance. Performance of the assay was calculated and the Z' factors were ≥ 0.5 (23).

Drug Screen Assay in Hs 919.T. cell line

Drugs or vehicle (DMSO) were preloaded by the KU HTSL as 250 nL aliquots on an Echo550 platform to each well to give a final dose of 1 μM in 25 μl. Cells were grown to 80% confluence, harvested and aliquoted into 384 well plates at concentrations of 750 cells per well in a total volume of 25 μl/well using a Matrix Wellmate (Thermo Scientific). Cells were cultured for 72 hours at 37 °C. 25 μl CellTiter-Glo® Reagent was added directly to each well, the plates were incubated at room temperature for 15 min and the luminescence signal was measured. Following subtraction of background counts, the percentage of growth inhibition was calculated by dividing the value from drug-treated sample by that from control well incubated in the absence of drug. Samples exhibiting >50% growth inhibition in the presence of 1 μM drug were classified as positive hits.

TrxR Activity Measurement

Cells in log phase of growth were grown to 80% confluence, harvested and aliquoted into 6-well plates at concentrations of 500,000 cells per well in a total volume of 1 ml/well. Cells were allowed to attach overnight and were treated with or without auranofin or IM at indicated concentrations for 6 hours. Cells were harvested and 50 μg of total protein was used for each sample assessment. TrxR activity was measured using the TrxR Reductase Assay Kit (Abcam) per manufacturer's instructions.

ROS Activity Measurement

Cells in log phase of growth were grown to 80% confluence, harvested and aliquoted into 96 well plates at concentrations of 15,000 cells per well in a total volume of 100 μl/well. Cells were allowed to attach overnight. Cell were preloaded with 2',7'-dichlorodihydrofluorescin diacetate (DCFH-DA) for 30 min and treated with or without auranofin or IM at indicated concentrations for 6 hours. ROS activity was measured using the OxiSelectTM Intracellular ROS Assay Kit (Cell Biolabs, INC) per manufacturer's instructions.

Early Apoptosis Assay

Cells in log phase of growth were grown to 80% confluence, harvested and aliquoted into 6-well plates at a concentration of 5,000,000 cells per well in a total volume of 5 ml. Cells were allowed to attach overnight and then were treated with auranofin at different concentrations (0, 0.2% DMSO, 0.1 and 10 μM) for 24 h. Early apoptosis cells were detected by the Guava Nexin® Annexin V assay kit using Guava easyCyte™ sampling flow cytometer (Millipore).

Cell Proliferation and Caspase 3/7 Activity Assay

Cells in log phase of growth were grown to 80% confluence, harvested and aliquoted into 384-well plates at concentrations of 1,000–1,500 cells per well in a total volume of 20 μl/well using a Matix Wellmate (Thermo Scientific). Cells were allowed to attach overnight and 5 μl of culture media containing either vehicles or drug were added to each well. Cell proliferation was evaluated. After reading fluorescence, Caspase-Glo® 3/7 Assay Reagent (Promega) was used according to manufacturer's instructions. After background subtraction,

NIH-PA Author Manuscript

NIH-PA Author Manuscript

NIH-PA Author Manuscript

luminescence was measured and quantified by normalizing luminescence to fluorescence. Caspase 3/7 activity values were expressed as percentage of the mean of the relative vehicle controls.

Western Blot Analysis

Cells in log phase of growth were grown to 80% confluence, harvested and aliquoted into 6-well plates at a concentration of 5,000,000 cells per well in a total volume of 5 ml. Cells were allowed to attach overnight and then were treated with drugs at indicated doses for 6 hours. Whole-cell extract was prepared as described previously (14). Briefly, for each specimen, 50 μg whole-cell extract was electrophoresed on 10% precast polyacrylamide gel (Bio-Rad) and transferred onto nitrocellulose membranes. After 1-hour blocking in 5% bovine serum albumin (BSA) or 5% nonfat milk in TBS/0.1% Tween-20, membranes were incubated with primary antibodies (1:1,000 or 1:500 dilution) overnight at 4 °C. After incubation with HRP-conjugated secondary antibody at room temperature for 1 hour, development was carried out using Immun-Star™ HRP Chemiluminescence Kits (Bio-Rad). All western blots were performed in triplicate. Phosphorylated proteins were normalized to total proteins and quantified using Image J (NIH).

Antibodies

The following antibodies were used for Western blot analysis: rabbit anti-c-KIT, rabbit anti-c-KIT XP®, rabbit anti-phospho-c-KIT (Tyr719), rabbit anti-AKT, rabbit anti-phospho-AKT (Ser473) XP®, rabbit anti-phospho-AKT (Thr308), mouse anti-ERK1/2, mouse anti-phospho-ERK1/2 (Thr202/Tyr204) (Cell Signaling technology, MA); mouse anti-β-actin (Sigma, MO).

Statistics

Data were reported as mean ± SEM of 3–5 independent experiments, each treatment was performed in duplicate or triplicate. Values were compared using the Student's *t* test or with one-way ANOVA when three groups were present. Results were deemed statistical significant if $p < 0.05$.

RESULTS

Screening FDA Approved Drugs for Activity in GIST

To identify drugs that might be repurposed for patients with GIST, we used a quantitative drug screen experimental approach to assess the activity of 796 FDA-approved drugs in GISTs. The CellTiter-Blue® oxidation-reduction dye is used as an indicator of cell viability. Prior to the screen, the cell viability assay was miniaturized to a 384-well format to accelerate assay throughput. For optimization of assay performance, the number of cells/well and the length of the incubation period, and the volume of CellTiter-Blue reagent were empirically determined (Table 1). In order to reduce systematic errors such as variation in incubation time, time drift in measuring different plates, DMSO tolerance and edge effect were also considered and tested. Our DMSO tolerance assay indicates that the DMSO used in the screen does not affect cell viability (see supporting material, Figure S1A). In addition, the edge effect assay indicates that after 5 hours, the signal will have significant reduction in wells at edge (see supporting material, Figure S1B). Therefore, we controlled reading time to less than 5 hours for each cell line.

The protocol of the preliminary screening study is summarized in Table 1. A total of 152 plates were screened. The assay performed well over the entire course of the screen as demonstrated by the Z' values. The averaged signal/background ratio, Z' value and the signal

NIH-PA Author Manuscript

NIH-PA Author Manuscript

NIH-PA Author Manuscript

window of the control wells for each cell line were summarized in supporting material Table S2.

Data were normalized as percentage inhibition relative to vehicle control and plotted in a 3-D plot (Figure 1A) for each plate. Curves were classified into 3 categories (supporting material Table S3 and Figure 1B, 1C & 1D) and IC_{50} values were calculated and both of them were used to define active/inactive drugs. FDA-approved drugs failing to demonstrate activity were ruled out from the following analysis. IC_{50} values were calculated for drugs demonstrating positive inhibition values (IC_{50} value < 1.0 μM). Typical IC_{50} curves were shown in Figure 1E.

Based on drug concentration-response curve quality in the primary screen, 29 drugs showed preclinical potent *in vitro* activity ($IC_{50} \leq 1$ μM) against one or more GIST cell lines including two mutant GIST cell lines (GIST-T1, exon 11 *KIT* mutation, and GIST 882, exon 13 *KIT* mutation), and an imatinib resistant variant of T1 cell line (GIST T1-10R, derived in the Godwin laboratory). The screen results are summarized in Table 2.

Validating Activity of FDA Approved Drugs in GIST

The active compounds from the screen were triaged into 3 groups: active in i) one of the GIST cell lines, ii) two of the GIST cell lines, or iii) three GIST cell lines (Table 2). The ideal candidate should have a low IC_{50} value of < 1.0 μM against three GIST cell lines and a high IC_{50} value of > 1.0 μM against the ULTR cell line. However, later we found the data generated from ULTR cell line are not informative, since these cells were also transformed (data not shown). Instead, Hs 919.T., a benign osteoid osteoma cell line, was used as the non-sarcoma cell line control. Drugs were screened at the concentration of 1 μM. The data are summarized in Table S4 in the supplemental materials. Ten drugs (bortezomib, doxorubicin, mitoxantrone, idarubicin HCl, digoxin, daunorubicin, vinorelbine, plicamycin, dactinomycin and mebendazol) showed inhibition against Hs 919.T. cell proliferation greater than 50% indicating that these drugs have no selectivity against sarcoma and non-sarcoma cells. Therefore, based on inhibitory activity against three GIST cell lines, and subsequent drug development and regulatory science gap analysis of each of the 29 screening hits, three drugs (auranofin, bortezomib, and idarubicin) which are active in all GIST cell lines and one drug (fludarabine phosphate) which is active in IM-resistance cell line were prioritized for further validation. Pure compounds (> 99% purity) were obtained and prepared as described in the materials and methods section. *In vitro* activities of the four prioritized drugs were evaluated employing 12-point dose-response curves ranging from 20 μM to 1 nM, with triplicate sampling. Typical IC_{50} curves generated from the validation are shown in Figure 1F. The structures of the candidate drugs are summarized in Table S5. The IC_{50} values and drug selectivity were confirmed and listed in Table 3. The hit validation of the top candidates was highly reproducible except fludarabine phosphate showed active across the three GIST cell lines.

Two drugs, auranofin and fludarabine phosphate showed selectivity against GIST cell lines. One of them, auranofin, has been shown to inhibit TrxR system and has been proposed as a promising experimental agent for cancer treatment (20, 24, 25). The Auranofin pharmacological data is listed in Table S6. Auranofin has an acceptable clinical safety profile (26) and is currently being evaluated in chronic lymphocytic leukemia patients at the University of Kansas Cancer Center, National Heart, Lung and Blood Institute, and The Ohio State University Comprehensive Cancer Center (ClinicalTrials.Gov Identifier NCT01419691). Furthermore, we analyzed a microarray dataset GSE31802 (27) for GIST tumors and found that the TrxR (all three isoforms TrxR1, TrxR2, TrxR3) are present in specimens from GIST patients (n=14) with expression of TrxR1 and TrxR3 being 1.2 folds higher (p value< 0.01) as compared to that of TrxR2 (Figure S2A & S2B). Based on our

NIH-PA Author Manuscript

NIH-PA Author Manuscript

NIH-PA Author Manuscript

findings, prior human safety experience, as well as activity of this FDA approved drug in other cancers, we selected auranofin for further mechanistic studies in GIST.

Auranofin Inhibits TrxR Enzymatic Activity in GIST Cells

Gold(I) and gold(III) compounds have been reported to be highly specific inhibitors of mitochondrial TrxR. It has been shown that gold compounds preferentially interact with a selenol group in the active site at the C terminus of TrxR since selenol displays a greater affinity toward heavy metals (28). Mammalian TrxR is a key enzyme for maintenance of the intracellular reduced environment. Impaired TrxR system will lead to increased levels of oxidized thioredoxin that will render its ability to protect cells from a variety of oxidative stresses (28). As such, we hypothesized that TrxR might be a molecular target of auranofin treatment in GIST cells. To examine whether auranofin treatment affects the TrxR/Trx system in GIST cells, we compared levels of TrxR activity after auranofin and IM treatments. Figure 2A shows the effect of a 6-hour auranofin treatment on GIST cells. Only GIST T1-10R cells showed a significant decrease of TrxR activity at the lower concentration treatment (0.01 and 0.1 μM). At higher concentrations (1.0 and 10 μM), auranofin dramatically reduces the TrxR activity in all three GIST cell lines. At auranofin exposures in cell culture up to 24 hours at 1 μM, TrxR enzymatic activity is inhibited (Figure S3A, B & C). Compared to auranofin treatments, IM treatments did not change the TrxR activity level in all three GIST cell lines (Figure 2B).

Auranofin Increases Intracellular ROS Levels in GIST Cells

It is known that all types of cells generate low but detectable amounts of ROS under different circumstances and that ROS serve as important mediators of redox homeostasis under physiological conditions. The production of ROS is tightly regulated by antioxidant systems, which maintain redox homeostasis within the cellular environment. Over-production of ROS and impaired antioxidant systems (e.g., TrxR system) may lead to oxidative stress and it is known to contribute to the pathogenesis of several diseases including cancers (24, 25). It is also known that ROS have distinct functional effects, which are dependent on a number of factors such as the type of cell within which ROS are generated, and the local concentration of ROS at subcellular sites where they may modulate enzyme activity and influence gene expression (29, 30).

The effect of auranofin on the production of ROS in GIST cells is shown in Figure 2C. The addition of auranofin (1 and 10 μM) strongly stimulates the formation of ROS in GIST-T1 and GIST T1-10R cells (2.4-fold and 2.6-fold changes, respectively, Figure 2C). Compared to the other two GIST cell lines, GIST 882 cell line did respond to auranofin treatment at the concentration of 1 and 10 μM but the decrease in the ROS production was relatively lower (1.5-fold change, Figure 2C). At lower concentrations (0.01 and 0.1 μM auranofin treatment), ROS remained relatively stable in all three GIST cell lines. As we expected, the longer treatment with auranofin induces higher production of ROS in all three GIST cell lines (Figure S3D, E & F), while IM treatment had little effect on ROS (Figure 2D).

Effect of Auranofin on PI3K, AKT and ERK1/2 Pathways in GIST Cells

GIST-T1 and GIST 882 cell lines demonstrate constitutive activation of the AKT and ERK1/2 pathways and exposure to IM resulted in dephosphorylation of KIT, AKT and ERK1/2 (14). It has been shown that oxidation of thioredoxin or increased ROS may trigger the activation of ERK pathway depending on the transient or prolonged activation (31, 32). Under basal or low oxidative stress, ROS may promote cell survival and proliferation which leads to cancer development (33). Excessive ROS levels, however, can cause cellular damage, and even cell death (34). It is also known that the effect of ROS is cell-type dependent (35–38). In order to understand the mechanism of action of auranofin in GIST

NIH-PA Author Manuscript

NIH-PA Author Manuscript

NIH-PA Author Manuscript

cells, it is important to identify these molecular components involved in the cascade of events that finally trigger cell death. Therefore, we examined whether PI3K, AKT and ERK signaling pathways were involved in auranofin treatment in GIST cells. Our results indicate the effect of auranofin on PI3K, AKT and ERK signaling pathways in GIST cells is dose- and cell-type dependent. These observations are consistent with our TrxR and ROS activity results. Treatments of 0.01 or 0.1 μM auranofin for 6 hours resulted in a basal or low level of ROS which leads to the increasing of $pAKT^{Thr308}$ levels (~8-fold, ~ 5-fold respectively, Figure 3B&E) in GIST-T1 cells. When cells were treated with 1 or 10 μM auranofin for 6 hours, which resulted in higher fold changes of ROS production (~2.0-fold-change, Figure 2C) in GIST-T1 cells, p-cKT, $pAKT^{Ser473}$, and $pAKT^{Thr308}$ levels are all decreased (~0.5-fold change, ~0.5-fold change, and ~0.06-fold-change respectively, Figure 3B&E). Similar to GIST-T1 cells, GIST T1-10R cells respond to auranofin in a manner related to ROS levels. Treatments of 0.01 or 0.1 μM auranofin for 6 hours resulted in the increasing pERK1/2 levels (~3.0-fold and ~3.6-fold changes, Figure 3C&F). Treatments of 1 or 010 μM auranofin for 6 hours resulted in the decreasing of $pAKT^{Thr308}$ levels (~0.6-fold and ~0.4-fold changes, Figure 3C&F) and the increasing pERK1/2 levels (~2.7-fold and ~2.4-fold changes, Figure 3C&F). GIST 882 cell line generates different levels of ROS and is more stable compared to vehicle-treated cells across all auranofin treatments (~1.5-fold change, Figure 2C), therefore, auranofin does not noticeably alter phosphorylated levels of cKIT, AKT and ERK (Figure 3A&D).

Auranofin Stimulates Early Apoptosis and Caspase 3/7 Activity which Causes Reduction in Cell Viability in GIST Cells

To test our hypothesis that auranofin treatment in GIST cells inhibits TrxR enzymatic activity and increases ROS production leading to apoptosis (Figure 3G), we carried out early apoptosis detection assay using Annexin V staining. The fraction of early apoptotic cells increased ~4-fold, ~2.8-fold, and ~2.3-fold in GIST-T1, GIST T1-10R and GIST 882 cells respectively after the 24-h auranofin treatment (1 μM) (Figure S4). To further study the apoptotic affect by auranofin treatment, we carried out caspase 3/7 activity assays and cell viability assays. The apoptotic activity of auranofin was evaluated on GIST cells with the presence of 0.1 and 1 μM auranofin for 72 hours. Auranofin treatment was able to increase Caspase 3/7 activity (Figure 3H). Caspase 3/7 is responsible for cleavage of cellular proteins that are characteristically proteolysed during apoptosis. After 72 hour of treatment, the percentage of living cells was determined and is shown in Figure 3I. As described in Figure 3H, auranofin induced a decrease in cell viability after 1 μM treatment in all three GIST cell lines. It is very interesting that low-dose auranofin treatment also induced cell proliferation in GIST-T1 and GIST T1-10R cells (~1.1–1.2 fold, Figure 3I).

DISCUSSION

The drug screening assay described in the present study is robust and meets criteria for industry-accepted high-throughput screening standards ($Z' > 0.5$) (Table S2), therefore, this protocol can easily be applied to higher throughput analysis. Of the 796 FDA-approved compounds screened, 29 were demonstrated to possess inhibitory properties against one or more GIST cell lines with an IC_{50} value equal to or lower than 1 μM. Of these, four compounds were selected as those representing the most promising starting points for further validation, since they had activity across both IM-sensitive and -resistant GISTs (Table 3). Validation confirmed the activity and selectivity of these drugs. The different results between the primary screen and validation for fludarabine phosphate suggest that the drug may have been preloaded incorrectly using the Echo550 platform, leading to the initial under appreciation of its activity in the primary screen.

NIH-PA Author Manuscript

NIH-PA Author Manuscript

NIH-PA Author Manuscript

One of the hits, auranofin (Ridaura®), is an oral, lipophilic gold-containing compound approved by the FDA in 1985 for the treatment of rheumatoid arthritis. Auranofin has multiple cellular effects that contribute to its efficacy as an anti-arthritis agent. It inhibits TrxR and induces a permeability transition resulting in cytochrome c release from the mitochondria, leading to apoptotic cell death (29, 38–40). In HL-60 human promyelocytic leukemia cells, reactive oxygen species (ROS) – induced apoptosis is dependent on p38-MAPK signaling (41). It also induces G2 cell cycle arrest, consistent with activation of a DNA damage-responsive checkpoint (42). In addition, auranofin modulates multiple signaling pathways that are critical to cancer cell survival. It inhibits JAK/STAT signaling, reducing the levels of the anti-apoptotic protein Mcl-1(30), reduces levels of NF-kB transactivated anti-apoptotic proteins (30, 43), antagonizes EGF ligand-receptor interactions (44), and blocks the activity of protein kinase C (45). There is evidence that low levels of oxidants activate several cell signaling pathways and regulate cell survival and proliferation, whereas high levels of oxidants stimulate stress-activated signaling pathways leading to cell death (35–37). However, the effect of ROS is cell type dependent (46). The results of our experiments show a dose-dependent inhibition of TrxR activity and ROS production in the auranofin concentration range of 0.01 to 10 μM. The response to auranofin treatment in GIST cell lines is closely related to the endogenous or inducible ROS level. The results clearly indicate that early apoptosis was induced by auranofin treatment and caspase 3/7 proteases are activated in response to apoptosis induced by auranofin in all GIST cell lines. These results provide the preclinical proof-of-principle to explore the use of auranofin in the oncology setting.

Auranofin is effective and well tolerated in rheumatoid arthritis. In dose titration studies, auranofin showed activity at doses as low as 2 mg orally daily, with greater efficacy at 6 and 9 mg daily (47–49). Daily doses greater than 6 mg led to more rapid clinical improvement. The most frequent side effects are diarrhea, rash and pruritis; stomatitis, alopecia and conjunctivitis (47, 49). Serious, but infrequent, side effects include anemia, leucopenia, thrombocytopenia, eosinophilia and proteinuria. All are reversible with dose reduction or discontinuation of therapy. Its safety in pregnant and lactating women has not been conclusively established. Results from this work are consistent with other investigators reporting that auranofin has potential anti-cancer effect through induction of apoptotic cell death in tumor cells (24, 28). Besides its potential anti-cancer activity, recently auranofin has been reported to have potential amebicidal activity and is being repurposed for the treatment of amebiasis (50).

The results obtained in this study support the idea that auranofin can induce apoptosis in GIST cells as a result of inhibition of TrxR and subsequent increases in intracellular levels of ROS. More importantly, the anti-cancer activity associated with auranofin may be independent of the mutational status and prior response to imatinib and may be more closely related to the endogenous and inducible levels of ROS (Figure 2 and data not shown). These preclinical data provide a strong rationale to evaluate auranofin in patients with treatment-refractory GIST.

The evaluation of potential new uses for FDA approved represents an opportunity to rapidly advance to cancer patients, promising drug therapies by capitalizing on existing data and experience. The same holds true for abandoned or “shelved” drug candidates. There is growing interest in partnering with innovator firms to potentially evaluate new uses for “shelved” drugs, the development of which have been “abandoned” due to issues other than drug safety. Weir, Austin and DeGennaro (20) reported the rapid translation of auranofin *in vitro* screening results in primary CLL cell lines directly into a multi-site, clinical proof of concept trial in chronic lymphocytic leukemia (CLL) patients (ClinicalTrials.Gov Identifier NCT01419691). As a result of the studies described in this publication, a drug repurposing

NIH-PA Author Manuscript

NIH-PA Author Manuscript

NIH-PA Author Manuscript

strategy is underway to rapidly translate these findings to GIST patients with recurrent and metastatic disease.

Supplementary Material

Refer to Web version on PubMed Central for supplementary material.

Acknowledgments

We would like to thank the KU Cancer Center's Lead Development and Optimization Shared Resource for providing the drug library and technical support. We would also like to acknowledge Dr. Anuradha Roy, Assistant Director of the KU HTSL, for help designing the HTS format. This work was supported in part by a grant from the NCI R01 CA106588 (A.K.G.) and the NIH (UL1 TR000001-02S1 to S.W. and A.K.G.), the KU Cancer Center's CCSG (P30 CA168524), and the Kansas Bioscience Authority Eminent Scholar Program.

The authors would also like to acknowledge support from the University of Kansas Cancer Center, the Kansas Bioscience Authority Eminent Scholar Program, the Chancellors Distinguished Chair in Biomedical Sciences endowment at KUMC, the Ewing Marion Kauffman Foundation, and University of Kansas Endowment Association.

Financial Support: This investigation was supported by grants from the NCI (R01 CA106588), the NIH (UL1 TR000001-02S1), the KU Cancer Center's CCSG (P30 CA168524), and the Kansas Bioscience Authority Eminent Scholar Program.

REFERENCES

1. Corless CL, Heinrich MC. Molecular pathobiology of gastrointestinal stromal sarcomas. Annu Rev Pathol. 2008; 3:557–86. [PubMed: 18039140]
2. Hirota S, Isozaki K, Moriyama Y, Hashimoto K, Nishida T, Ishiguro S, et al. Gain-of-function mutations of c-kit in human gastrointestinal stromal tumors. Science. 1998; 279:577–80. [PubMed: 9438854]
3. Heinrich MC, Corless CL, Duensing A, McGreevey L, Chen CJ, Joseph N, et al. PDGFRA activating mutations in gastrointestinal stromal tumors. Science. 2003; 299:708–10. [PubMed: 12522257]
4. Rink L, Godwin AK. Clinical and molecular characteristics of gastrointestinal stromal tumors in the pediatric and young adult population. Curr Oncol Rep. 2009; 11:314–21. [PubMed: 19508837]
5. Belinsky MG, Skorobogatko YV, Rink L, Pei J, Cai KQ, Vanderveer LA, et al. High density DNA array analysis reveals distinct genomic profiles in a subset of gastrointestinal stromal tumors. Genes Chromosomes Cancer. 2009; 48:886–96. [PubMed: 19585585]
6. Hostein I, Faur N, Primois C, Boury F, Denard J, Emile JF, et al. BRAF mutation status in gastrointestinal stromal tumors. Am J Clin Pathol. 2010; 133:141–8. [PubMed: 20023270]
7. Corless CL, Barnett CM, Heinrich MC. Gastrointestinal stromal tumours: origin and molecular oncology. Nat Rev Cancer. 2011; 11:865–78. [PubMed: 22089421]
8. Antonescu CR. The GIST paradigm: lessons for other kinase-driven cancers. J Pathol. 2011; 223:251–61. [PubMed: 21125679]
9. Blay JY, von Mehren M, Blackstein ME. Perspective on updated treatment guidelines for patients with gastrointestinal stromal tumors. Cancer. 2010; 116:5126–37. [PubMed: 20661913]
10. Yang J, Du X, Lazar AJ, Pollock R, Hunt K, Chen K, et al. Genetic aberrations of gastrointestinal stromal tumors. Cancer. 2008; 113:1532–43. [PubMed: 18671247]
11. Gounder MM, Maki RG. Molecular basis for primary and secondary tyrosine kinase inhibitor resistance in gastrointestinal stromal tumor. Cancer Chemother Pharmacol. 2011; 67(Suppl 1):S25–43. [PubMed: 21116624]
12. Heinrich MC, Corless CL, Blanke CD, Demetri GD, Joensuu H, Roberts PJ, et al. Molecular correlates of imatinib resistance in gastrointestinal stromal tumors. J Clin Oncol. 2006; 24:4764–74. [PubMed: 16954519]

NIH-PA Author Manuscript

NIH-PA Author Manuscript

NIH-PA Author Manuscript

13. van Glabbeke M, Verweij J, Casali P, Le Cesne A, Hohenberger P, Ray-Coquard I, et al. Initial and Late Resistance to Imatinib in Advanced Gastrointestinal Stromal Tumors Are Predicted by Different Prognostic Factors: A European Organisation for Research and Treatment of Cancer - Italian Sarcoma Group - Australasian Gastrointestinal Trials Group Study. J Clin Oncol. 2005; 23:5795–804. [PubMed: 16110036]

14. Tarn C, Skorobogatko YV, Taguchi T, Eisenberg B, von Mehren M, Godwin AK. Therapeutic effect of imatinib in gastrointestinal stromal tumors: AKT signaling dependent and independent mechanisms. Cancer Res. 2006; 66:5477–86. [PubMed: 16707477]

15. Dupart JJ, Trent JC, Lee HY, Hess KR, Godwin AK, Taguchi T, et al. Insulin-like growth factor binding protein-3 has dual effects on gastrointestinal stromal tumor cell viability and sensitivity to the anti-tumor effects of imatinib mesylate in vitro. Mol Cancer. 2009; 8:99. [PubMed: 19903356]

16. Bardsley MR, Horvath VJ, Asuzu DT, Lorincz A, Redelman D, Hayashi Y, et al. Kitlow stem cells cause resistance to Kit/platelet-derived growth factor alpha inhibitors in murine gastrointestinal stromal tumors. Gastroenterology. 2010; 139:942–52. [PubMed: 20621681]

17. Lorincz A, Redelman D, Horvath VJ, Bardsley MR, Chen H, Ordog T. Progenitors of interstitial cells of cajal in the postnatal murine stomach. Gastroenterology. 2008; 134:1083–93. [PubMed: 18395089]

18. Godwin AK. Bench to bedside and back again: personalizing treatment for patients with GIST. Mol Cancer Ther. 2011; 10:2026–7. [PubMed: 22072810]

19. Chong CR, Sullivan DJ Jr. New uses for old drugs. Nature. 2007; 448:645–6. [PubMed: 17687303]

20. Weir SJ, DeGennaro LJ, Austin CP. Repurposing approved and abandoned drugs for the treatment and prevention of cancer through public-private partnership. Cancer Res. 2012; 72:1055–8. [PubMed: 22246671]

21. Frolov A, Chahwan S, Ochs M, Arnoletti JP, Pan ZZ, Favorova O, et al. Response markers and the molecular mechanisms of action of Gleevec in gastrointestinal stromal tumors. Mol Cancer Ther. 2003; 2:699–709. [PubMed: 12939459]

22. Tuveson DA, Willis NA, Jacks T, Griffin JD, Singer S, Fletcher CD, et al. STI571 inactivation of the gastrointestinal stromal tumor c-KIT oncoprotein: biological and clinical implications. Oncogene. 2001; 20:5054–8. [PubMed: 11526490]

23. Inglese J, Shamu CE, Guy RK. Reporting data from high-throughput screening of small-molecule libraries. Nat Chem Biol. 2007; 3:438–41. [PubMed: 17637769]

24. Casini A, Messori L. Molecular mechanisms and proposed targets for selected anticancer gold compounds. Curr Top Med Chem. 2011; 11:2647–60. [PubMed: 22039866]

25. Gandin V, Fernandes AP, Rigobello MP, Dani B, Sorrentino F, Tisato F, et al. Cancer cell death induced by phosphine gold(I) compounds targeting thioredoxin reductase. Biochemical pharmacology. 2010; 79:90–101. [PubMed: 19665452]

26. Felson DT, Anderson JJ, Meenan RF. The comparative efficacy and toxicity of second-line drugs in rheumatoid arthritis. Results of two metaanalyses. Arthritis Rheum. 1990; 33:1449–61.

27. Niinuma T, Suzuki H, Nojima M, Nosho K, Yamamoto H, Takamaru H, et al. Upregulation of miR-196a and HOTAIR drive malignant character in gastrointestinal stromal tumors. Cancer Res. 2012; 72:1126–36. [PubMed: 22258453]

28. Saggioro D, Rigobello MP, Paloschi L, Folda A, Moggach SA, Parsons S, et al. Gold(III)-dithiocarbamato complexes induce cancer cell death triggered by thioredoxin redox system inhibition and activation of ERK pathway. Chem Biol. 2007; 14:1128–39. [PubMed: 17961825]

29. Rigobello MP, Bindoli A. Mitochondrial thioredoxin reductase purification, inhibitor studies, and role in cell signaling. Methods Enzymol. 2010; 474:109–22. [PubMed: 20609907]

30. Nakaya A, Sagawa M, Muto A, Uchida H, Ikeda Y, Kizaki M. The gold compound auranofin induces apoptosis of human multiple myeloma cells through both down-regulation of STAT3 and inhibition of NF-kappaB activity. Leuk Res. 2011; 35:243–9. [PubMed: 20542334]

31. Zhang R, Al-Lamki R, Bai L, Streb JW, Miano JM, Bradley J, et al. Thioredoxin-2 inhibits mitochondria-located ASK1-mediated apoptosis in a JNK-independent manner. Circ Res. 2004; 94:1483–91. [PubMed: 15117824]

NIH-PA Author Manuscript

NIH-PA Author Manuscript

NIH-PA Author Manuscript

32. Kim MR, Chang HS, Kim BH, Kim S, Baek SH, Kim JH, et al. Involvements of mitochondrial thioredoxin reductase (TrxR2) in cell proliferation. Biochem Biophys Res Commun. 2003; 304:119–24. [PubMed: 12705894]
33. Burdon RH. Superoxide and hydrogen peroxide in relation to mammalian cell proliferation. Free Radic Biol Med. 1995; 18:775–94. [PubMed: 7750801]
34. Trachootham D, Lu W, Ogasawara MA, Nilsa RD, Huang P. Redox regulation of cell survival. Antioxid Redox Signal. 2008; 10:1343–74. [PubMed: 18522489]
35. Kim JH, Choi W, Lee JH, Jeon SJ, Choi YH, Kim BW, et al. Astaxanthin inhibits H2O2-mediated apoptotic cell death in mouse neural progenitor cells via modulation of P38 and MEK signaling pathways. J Microbiol Biotechnol. 2009; 19:1355–63. [PubMed: 19996687]
36. Giorgio M, Trinei M, Migliaccio E, Pelicci PG. Hydrogen peroxide: a metabolic by-product or a common mediator of ageing signals? Nat Rev Mol Cell Biol. 2007; 8:722–8. [PubMed: 17700625]
37. Stone JR, Yang S. Hydrogen peroxide: a signaling messenger. Antioxid Redox Signal. 2006; 8:243–70. [PubMed: 16677071]
38. Rigobello MP, Callegaro MT, Barzon E, Benetti M, Bindoli A. Purification of mitochondrial thioredoxin reductase and its involvement in the redox regulation of membrane permeability. Free Radic Biol Med. 1998; 24:370–6. [PubMed: 9433913]
39. Rigobello MP, Folda A, Baldoin MC, Scutari G, Bindoli A. Effect of auranofin on the mitochondrial generation of hydrogen peroxide. Role of thioredoxin reductase. Free Radic Res. 2005; 39:687–95. [PubMed: 16036347]
40. Liu JJ, Liu Q, Wei HL, Yi J, Zhao HS, Gao LP. Inhibition of thioredoxin reductase by auranofin induces apoptosis in adriamycin-resistant human K562 chronic myeloid leukemia cells. Pharmazie. 2011; 66:440–4. [PubMed: 21699084]
41. Park SJ, Kim IS. The role of p38 MAPK activation in auranofin-induced apoptosis of human promyelocytic leukaemia HL-60 cells. British journal of pharmacology. 2005; 146:506–13. [PubMed: 16086031]
42. Glennas A, Rugstad HE. Ploidity and cell cycle progression during treatment with gold chloride, auranofin and sodium aurothiomalate. Studies on a human epithelial cell line and its sub-strains made resistant to the antiproliferative effects of these gold compounds. Virchows Arch B Cell Pathol Incl Mol Pathol. 1985; 49:385–93. [PubMed: 2867637]
43. Jeon KI, Jeong JY, Jue DM. Thiol-reactive metal compounds inhibit NF-kappa B activation by blocking I kappa B kinase. J Immunol. 2000; 164:5981–9. [PubMed: 10820281]
44. Froscio M, Murray AW, Hurst NP. Inhibition of epidermal growth factor binding to HeLa cells by auranofin. Biochemical pharmacology. 1987; 36:769–72. [PubMed: 3493779]
45. Froscio M, Murray AW, Hurst NP. Inhibition of protein kinase C activity by the antirheumatic drug auranofin. Biochemical pharmacology. 1989; 38:2087–9. [PubMed: 2735946]
46. Rao GN, Berk BC. Active oxygen species stimulate vascular smooth muscle cell growth and proto-oncogene expression. Circ Res. 1992; 70:593–9. [PubMed: 1371430]
47. Champion GD, Cairns DR, Bieri D, Adena MA, Browne CD, Cohen ML, et al. Dose response studies and longterm evaluation of auranofin in rheumatoid arthritis. J Rheumatol. 1988; 15:28–34. [PubMed: 3280795]
48. Williams HJ, Ward JR, Egger MJ, Reading JC, Samuelson CO, Altz-Smith M, et al. Auranofin, gold sodium thiomalate, and placebo in the treatment of rheumatoid arthritis. Cooperative systematic studies of rheumatic diseases. Clin Rheumatol. 1984; 3(Suppl 1):39–50. [PubMed: 6432412]
49. Furst DE. Mechanism of action, pharmacology, clinical efficacy and side effects of auranofin. An orally administered organic gold compound for the treatment of rheumatoid arthritis. Pharmacotherapy. 1983; 3:284–98. [PubMed: 6417628]
50. Debnath A, Parsonage D, Andrade RM, He C, Cobo ER, Hirata K, et al. A high-throughput drug screen for Entamoeba histolytica identifies a new lead and target. Nat Med. 2012

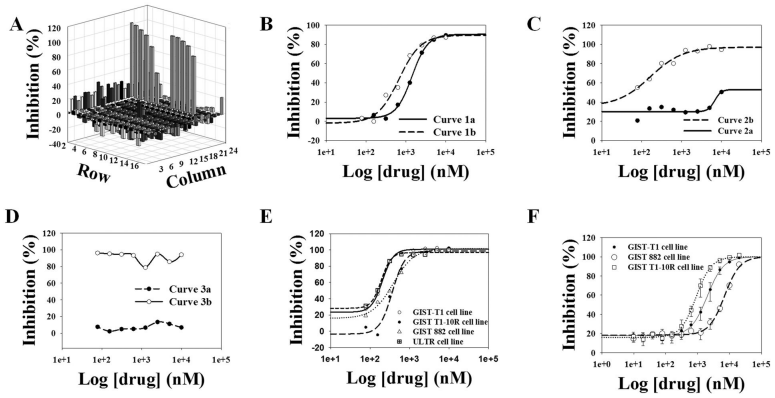

Figure 1.

Post-HTS analysis. A, data acquisition are shown as a 3-dimensional representation. Plot was generated from GIST T1-10R cell line. B, C and D, examples of drug concentration-response curves. Detailed information of curves are summarized in Table S3. E and F, IC_{50} curves for auranofin derived from the primary screen and derived from the subsequent validation assays.

NIH-PA Author Manuscript
NIH-PA Author Manuscript
NIH-PA Author Manuscript

NIH-PA Author Manuscript

NIH-PA Author Manuscript

NIH-PA Author Manuscript

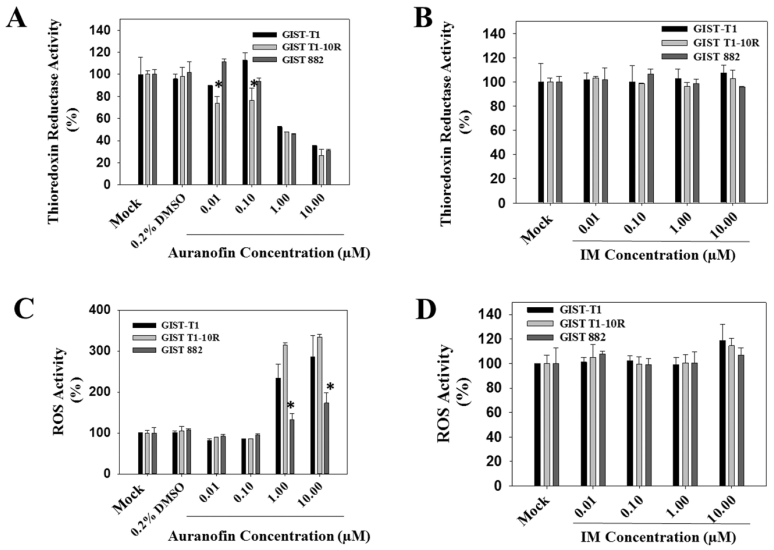

Figure 2.

In vitro effects of auranofin or IM treatment on TrxR/Trx system. A and B, auranofin inhibits thioredoxin reductase (TrxR) activity in GIST cells. IM does not alter TrxR activity. GIST cells were treated for 6 h with the indicated concentration of auranofin before cells were harvested and lysed. For each sample, 50 μg of protein cell lysate was assessed for TrxR activity by measuring NADPH-dependent reduction of DTNB. C and D, auranofin increases reactive oxygen species (ROS) activity in GIST cells. IM does not increase the production of ROS. GIST cells in a 96-well plate were pretreated with 1 mM DCFH-DA for 60 minutes at 37 °C. Cells were then treated for 6 h with the indicated concentration of auranofin. ROS activity was measured using DCF fluorescence. (* p value < 0.05)

NIH-PA Author Manuscript

NIH-PA Author Manuscript

NIH-PA Author Manuscript

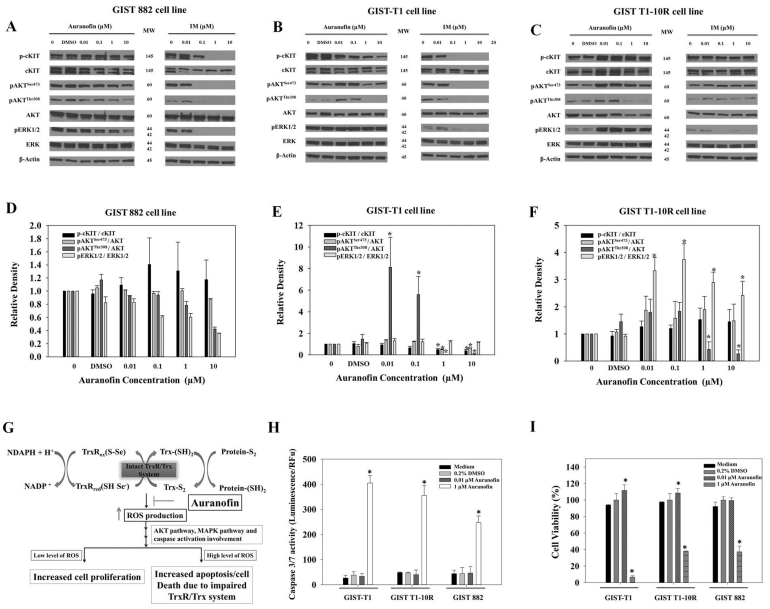

Figure 3.

Effect of auranofin or IM treatments on signaling pathways and cell viability. A, GIST 882. B, GIST-T1; and C, GIST T1-10R cells were treated with auranofin or IM at indicated concentration for 6 h. For each sample, 50 μg of total protein cell lysate was loaded for western blots. D, E, and F, Bar graph shows combined densitometric quantification (Image J) of western blot results. Each bar represents results from two independent experiments. G, proposed mechanism of auranofin action in GIST cells. Auranofin inhibits TrxR system and results in increased ROS production which finally leads to apoptosis and cell growth inhibition. H, Auranofin induces apoptosis in GIST cells. GIST cells in a 384-well plate were treated for 72 h with or without 0.01 μM or 1 μM of auranofin. Caspase 3/7 activity was measured by luminescence. F, Auranofin inhibits proliferation of GIST cells. GIST cells in a 384-well plate were treated for 72 h with or without 0.01 μM or 1 μM of auranofin. (* p value < 0.05)

NIH-PA Author Manuscript

NIH-PA Author Manuscript

NIH-PA Author Manuscript

Table 1

Automation protocol for drug repurposing screen.

Step	Event	Parameter	Description	Notes
1	Pre-spot library compoundsor DMSO	250 nl	Titration 10 μM to 0.7 μM (8 points)	Instrument: Echo 550
2	Add reagent	20 μl	GIST-T1 cells: 1,000 cells/well GIST 882 and GIST-T1-10R cells: 1,500 cells/well ULTR cells: 500 cells/well	Instrument: Matrix Wellmate
3	Incubate	72 hrs	5% CO_2/37 °C incubation	
4	Add reagent	5 μl	Promega CellTiter-Blue	
5	Incubate	3 hrs	5% CO_2/37 °C incubation	
6	Read	Fluorescence	544 nm Ex/590 nm Em, gain=70.	Instrument: Infinite M200 Pro

NIH-PA Author Manuscript
NIH-PA Author Manuscript
NIH-PA Author Manuscript

Table 2

Drug repurposing for GISTs hits summary.

Group	Drug	Therapeutic use	IC_{50} (μM)			
			GIST-T1	GIST 882	GIST TI-10R	ULTR
1	Albendazole	Anthelmintic	0.30	> 1.0	> 1.0	0.32
	Amsacrine	Antineoplastic, immune suppressive	0.31	> 1.0	> 1.0	> 1.0
	Mebendazole	Anthelmintic	0.81	> 1.0	> 1.0	0.73
	Paclitaxel	Antineoplastic	0.21	> 1.0	> 1.0	0.20
	Vinorelbine	Antineoplastic	0.23	> 1.0	> 1.0	0.08
	Chloroquine	Antimalaria	> 1.0	0.46	> 1.0	> 1.0
	Cladribine	Ant ine op lactic	> 1.0	0.76	> 1.0	0.54
	Danazol	Anterior pituitary suppressant	> 1.0	0.67	> 1.0	> 1.0
	Etoposide	Antineoplastic	> 1.0	0.03	> 1.0	> 1.0
	Teniposide	Antineoplastic	> 1.0	0.09	> 1.0	0.19
	Fludarabine Phosphate	Antineoplastic	> 1.0	> 1.0	0.81	> 1.0
2	Clofarabine	Antineoplastic, alkylating agent	> 1.0	0.99	> 1.0	0.18
	Dactinomycin	Antineoplastic, alkylating agent	0.07	<0.07 *	> 1.0	<0.07 *
	Daunorubicin	Antineoplastic	<0.07	0.17	> 1.0	<0.07 *
	Digitoxin	Inotropic, cardiotonic	<0.16	0.16	> 1.0	<0.07 *
	Doxorubicin	Antineoplastic	0.31	0.08	> 1.0	0.16
	Imatinib	Antineoplastic	0.18	0.13	> 1.0	> 1.0
	Mitoxantrone	Antineoplactic	0.42	0.08	> 1.0	<0.07 *
	Nilotimb	Antmeoplactic	0.38	0.10	> 1.0	> 1.0
	Plicamycin	Atineoplastic antibiotic	0.35	< 0.07 *	> 1.0	0.15
	Topotecan	Antineoplastic	0.08	0.44	> 1.0	0.09
3	Auranofin	Antirheumatic	0.23	0.38	0.16	0.19
	Bortezomib	Antimyeloma	<0.07 *	<0.07 *	0.50	<0.07 *
	Carbimazole	Antithyroid	<0.07 *	0.05	0.18	<0.07
	Digoxin	Cardiac stimulant	0.16	0.79	0.93	0.16
	Gentian Violet	Antibacterial, anthelmintic	0.52	0.25	0.96	0.16
	Idarubicin	Antileukemic	0.10	0.05	0.69	<0.07 *
	Ouabain	Antiarrhythmic, cardiotonic, hypertensive, Na/K ATPase inhibitor	0.21	0.03	0.24	<0.07 *

Compounds are listed alphabetically and not in order of activity.

Group 1 indicates drug activity (<1 μM) in a single GIST cell lines, Group 2 in two GIST cell lines, and Group 3 in all three GIST cell lines.

* IC50 < 0.07 μM and drug showed no dose response.

NIH-PA Author Manuscript

NIH-PA Author Manuscript

NIH-PA Author Manuscript

Table 3

Hit validation, drug structures and IC50 values of validated hits.

Drug	IC50			
	GIST-T1	GIST 882	GIST T1-10R	Hs 919.T.
IM	0.06 ± 0.03	0.13 ± 0.02	> 1	*ND
Auranofin	0.25 ± 0.15	0.64 ± 0.18	0.02 ± 0.01	*ND
Bortezomib	0.006 ± 0.002	0.002 ± 0.0003	0.001 ± 0.001	0.15 ± 0.01
Fludarabine Phosphate	0.53 ± 0.04	0.54 ± 0.03	0.84 ± 0.20	*ND
Idarubicin HC1	0.09 ± 0.01	0.13 ± 0.04	0.05 ± 0.01	0.07 ± 0.003

* ND: drugs showed no dose response.